Monitoring temperate glaciers: combined use of multi-date TerraSAR-X images and continous GPS measurements

Renaud Fallourd, Olivier Harant, Emmanuel Trouvé, Jean-Marie Nicolas, Florence Tupin, Michel Gay, Gabriel Vasile, Lionel Bombrun, Andrea Walpersdorf, Jonathan Serafini, et al.

MONITORING TEMPERATE GLACIER : COMBINED USE OF MULTI-DATE TERRASAR-X IMAGES AND CONTINUOUS GPS MEASUREMENTS

Renaud Fallourd[1,3], Olivier Harant[2,5], Emmanuel Trouvé[1], Jean-Marie Nicolas[3], Florence Tupin[3], Michel Gay[2], Gabriel Vasile[2], Lionel Bombrun[2], Andrea Walpersdorf[4], Jonathan Serafini[4], Nathalie Cotte[4], Luc Moreau[6] and Philippe Bolon[1]

[1] : Université de Savoie, Polytech'Savoie/LISTIC, 74944 Annecy-le-Vieux, France
Université de Savoie - Polytech'Savoie - BP 80439 - F-74944 Annecy-le-Vieux Cedex - FRANCE
{renaud.fallourd|emmanuel.trouve|philippe.bolon}@univ-savoie.fr
[2] : GIPSA-lab, CNRS - INP Grenoble, France
INPG CNRS - BP 46 - 38402 Saint-Martin-d'Hères - FRANCE
{olivier.harant|michel.gay|gabriel.vasile|lionel.bombrun}@gipsa-lab.inpg.fr
[3] : Institut Telecom, Telecom ParisTech, LTCI CNRS, 46 rue Barrault, 75013 Paris, France
LTCI CNRS - 46, Rue Barrault - 75013 Paris - FRANCE
{renaud.fallourd|jean-marie.nicolas|florence.tupin}@telecom-paristech.fr
[4] : LGIT, BP 53, 38041 Grenoble Cedex 9, France
BP 53 - 38041 Grenoble Cedex 9 - FRANCE
{andrea.walpersdorf|nathalie.cotte}@obs.ujf-grenoble.fr
[5] : IETR, CNRS Univ. Rennes 1, 263 Av du Général Leclerc, 35042 Rennes Cedex, France
CNRS - Univ. Rennes 1 - 263 Av du Général Leclerc - 35042 Rennes Cedex - FRANCE
olivier.harant@univ-rennes1.fr
[6] : EDYTEM, CNRS - Université de Savoie, F-73376 Le Bourget du Lac Cedex, France
CNRS - Université de Savoie - F-73376 Le Bourget du Lac Cedex - FRANCE

ABSTRACT

This paper highlights the contribution of TerraSAR-X (TSX) High Resolution (HR) images for temperate glacier monitoring. A series of 14 images have been acquired since October 2007 on the Mont-Blanc test area. This area involves well-known temperate glaciers which have been monitored and instrumented ("stick" for annual displacement/ablation, GPS, cavitometer for basal displacement...) for more than 50 years. The combined use of *in-situ* measurements and multi-temporal images allows to improve the potential of HR SAR measurements. Interpretation of HR images, investigation of interferometric and *correlation methods*, and the first glacier displacement results are presented.

1   INTRODUCTION

In the context of global warming, the monitoring of temperate glaciers is an important issue for economical and security reasons (water resources, falling ices...) and climate change monitoring. Due to the difficult access of many glacier areas, especially in Himalaya, and the environmental hazard, remotely sensed data are an attractive alternative of *in-situ* measurements. Furthermore, only a few sites are instrumented in the world and it is not possible to visit every glacier regularly. Therefore, compared to sparse terrestrial ground measurements, remote sensing is expected to provide dense measurements of physical parameters which are necessary to detect significant changes and to constrain glacier flow model. High resolution optical images have already allowed to measure the glacier topography and summer displacement[1]. Nevertheless, winter snowfall and clouds make optical correlation most of the year impossible. On this point, SAR (Synthetic Aperture Radar) data are a complementary information source which can be exploited during the cold season when reduced surface changes make SAR interferometry (InSAR) feasible [2].

Validating the SAR displacement measurements requires a ground truth. In this sense, the Chamonix Mont-Blanc test area which includes well-known glaciers such as the Mer de Glace glacier (the fourth European largest glacier complex) and the Argentière glacier, represents a perfect test-site. Both glaciers have been monitored and instrumented for several decades by different scientific teams. The Argentière glacier has been instrumented with a corner reflector (CR) provided by the DLR and a continuously recording GPS station. They have been installed in the upper part of the glacier (catchment area) during the second E-SAR campaign performed over this test-site in

February 2007 [3]. Combining this ground information with high spatial resolution images and the relatively short repeat cycle of TSX satellite (11 days) allows new investigations over moving glacier surfaces.

This paper presents the first analysis and results with the TSX data collection acquired over the Mont-Blanc area. To start with, an analysis of the amplitude images shows TSX improvement compared to the previous SAR sensors. Furthermore, the assessment of DInSAR (Differential interferometry) measurement potential is undertaken. Both points reveal that texture tracking method is a good alternative to estimate glacier displacement with TerraSAR-X images. Then, after a brief overview of texture tracking methods to estimate displacement in SAR images, the first displacement estimation results on Argentière glacier are presented. Finally, the accuracy of these first results are assessed by comparison with *in-situ* measurements.

Table 1. Stripmap descending TerraSAR-X acquisition over Chamonix Mont-Blanc test-site.

Date	Polarization	Pixel spacing		Incidence angle *(near-far)*
		Azimuth	Range	
2007-10-24	HH & VV	2.5 m	1.4 m	37.08° - 38.42°
2007-11-04	HH	1.5 m	0.9 m	35.96° - 38.54°
2008-01-09	"	"	"	"
2008-09-29	"	"	"	"
2008-10-10	"	"	"	"
2008-10-21	"	"	"	"
2009-01-06	HH & HV	2.5 m	1.4 m	37.08° - 38.42°
2009-01-17	"	"	"	"
2009-01-28	"	"	"	"
2009-02-08	"	"	"	"
2009-02-19	"	"	"	"
2009-03-02	"	"	"	"
2009-03-13	"	"	"	"
2009-03-24	"	"	"	"

2   ONE YEAR ANALYSIS OF TERRASAR-X IMAGES

In the framework of the TSX science project MTH0232 [4], a series of 14 TSX complex images has been acquired over the Chamonix Mont-Blanc test-site (from October 2007 to March 2009). Table 1 lists all of them with their polarization mode, pixel spacing and near-far range incidence angles. According to the number of polarimetric channels, single or dual polarization, the pixel spacing and size of range covered area change. Therefore the image collection covers the studied area over 18 months (2007.10.24 up to 2009.03.24) with different polarimetric channels (HH, HH/HV and HH/VV).
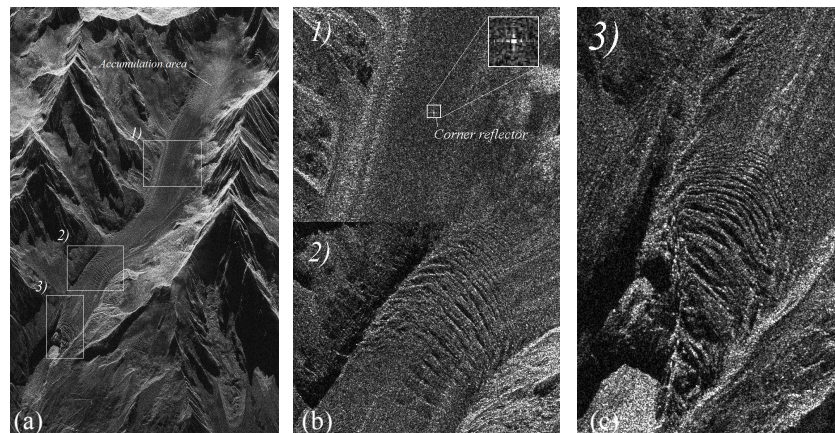

Figure 1. Amplitude image of Argentière glacier (2008-09-29). (a) Global view, (b) zoom on the corner reflector (CR) *1)* and cracked area *2)*, (c) zoom on "Lognan serac falls".

2.1 Contribution of High Resolution (HR)

TSX is the first civilian space-borne radar satellite allowing images with resolution close to one meter. The best pixel spacing, in Stripmap products, is respectively 1.5 m in azimuth and 0.9 m in range in single polarization mode. With such precision, it is possible to see more details than with previous space-borne SAR sensor images. Indeed, ass illustrated with Fig. 1, it is easy to discriminate between non-cracked and cracked parts, ablation and accumulation areas on Argentière glacier. In amplitude images, cracked zones appear as lines (succession of shadows and bright zone). The accumulation area (high density snow) appears with stronger backscattering coefficient than the ablation area.The corner reflector (Fig. 1-(b)), which has been installed in the upper part of the glacier d'Argentière, is totally visible in September/October 2008. Its intensity is about 40 dB higher than the local mean. In the other images, it is still visible but with a lower contrast due to slight orientation variation or snow accumulation.
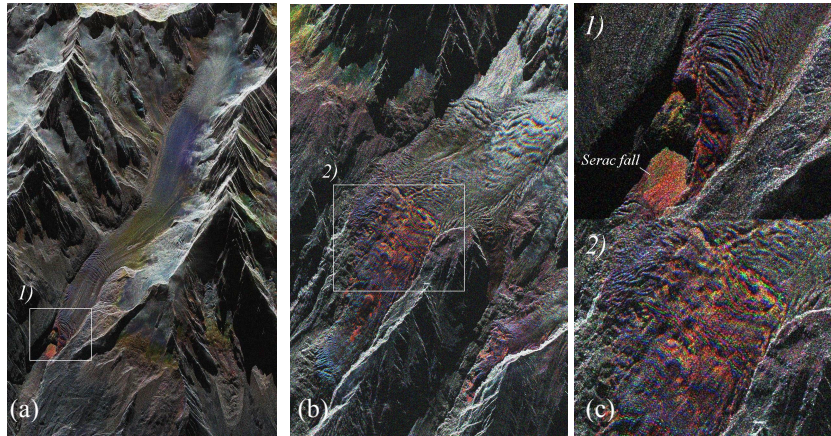

Figure 2. Red(2008-09-29)-Green(2008-10-10)-Blue(2008-10-21) composition image of Argentière glacier (a) and Bossons glacier (b). (c) Zoom on "Lognan serac falls" *1)* and fringes caused by displacement on Bossons glacier *2)*.

The main temporal evolutions can be observed by computing Red-Green-Blue (RGB) composition with 3 amplitude images which have been acquired at different dates. RGB composition reveals two main features: Serac falls and fast moving parts of the glacier. To illustrate it (Fig. 2-(a) and (b)), two RGB compositions of Argentière and Bossons glaciers are made with three images of autumn 2008 (red: 2008-09-29, green: 2008-10-10, blue: 2008-10-21).

On the one hand, serac falls create areas with ice blocks which increase ground roughness. Consequently, it increases the backscattered signal in this area. For example, Argentiere RGB composition shows a typical serac falls area just below the level of "Lognan serac falls" (see Fig. 2-(c)). This area appears red because of a serac fall which took place before 2008-09-29. Then, on two next dates, 11 and 22 days later, backscatterring decreases because of the ice blocks melting and settling. On the other hand, cracked fast moving parts of glaciers create red-green-blue fringes in RGB composition (see Fig. 2-(c)). At last, RGB composition emphasis the surface change of the upper part of Argentière glacier (Fig. 2-(a)): blue and yellow area just below the accumulation part. It appears that these two areas correspond to October 2008 snowfalls.

2.2 DInSAR potential

According to preliminary studies, TSX DInSAR measurements on temperate glacierised area are quite difficult because of the X-band ground texture sensibility, and ice surface changes during the 11-day interval of TSX repeat cycle [5] [6]. However, thanks to the resolution of TSX images, there is a hope to find valid interferometric pairs, depending on the surface cover and the registration accuracy on the moving parts. For example, a temperate glacier like Argentière presents in some areas a large number of stones and can move approximately 2 m/11 days. Considering data collection presented in Tab. 1, it is possible to make 9 interferometric couples with temporal baseline of 11 days: 2 in autumn 2008 and 7 in winter 2009. Obviously, the cold season is likely to provide the best DInSAR result because of reduced surface changes. Nonetheless X band is sensitive to snowfalls and snow settling due to gravity and mild spell.

Fig. 3 shows amplitude, coherence and phase of 2008-09-29/2008-10-10 interferometric couple. As expected, the two interferometric couples of autumn 2008 show the loss of coherence over the Argentière glacier. The high

coherence level parts correspond to altitude interval not yet covered by snow and where the forest is absent. Regardless, at this time of the year, several parts of "black" glaciers (surfaced by stones) such as Miage and Brenva glaciers present relatively high coherence, and useful phase information. In addition of stone surface, the relatively slow displacement of Miage glacier lower part (60 m/an) explains that this local coherence preservation can be observed in the middle of non moving area without specific registration.

Among 7 interferometric couples of winter 2009, only one works over the middle part of Argentière glacier: 2009-01-06/2009-01-17 couple. A long period with anti-cyclonic weather and cold temperature explains this result. Furthermore, it seems that these coherent parts coincide with stones on the glacier surface. On the contrary, all other couples don't work because of snowfalls and several mild spell in February and March 2009.
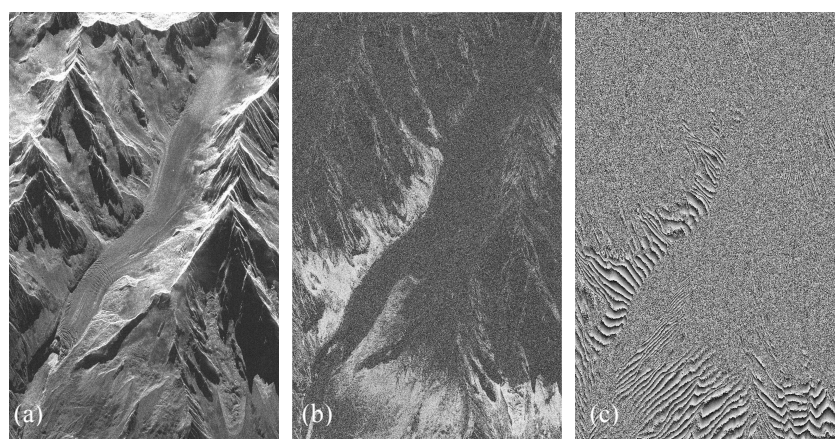

Figure 3. (a) Average amplitude image (5×5). DInSAR (b) coherence and (c) phase images calculated for 2008-09-29/2008-10-10 couple (baseline=139.2 m).

2.3 First conclusions

Visual investigations emphasize finesse and quality of TSX Stripmap image details. In relation to previous SAR sensors, the contribution on glacier environment examination is substantial: it improves the potential of SAR imagery for glacier monitoring as illustrated by the three images of autumn 2008 which allow a visual texture tracking of the glacier displacement. With a single valid interferometric couple on winter 2009, TSX DInSAR measurement potential seems to be compromised. It needs too specific conditions: no snowfalls, long period with anti-cyclonic weather, cold temperature... Up to now, it seems difficult to obtain interferometric series with TSX satellite because of its 11--day repeat cycle. In conclusion, to measure glacier displacement with TSX images, it is necessary to use alternative method to DinSAR. Visual analysis and the meter resolution justifies an exploration of tracking methods: cross-correlation and maximum likelihood texture tracking to estimate glacier displacement throughout the year.

3 DISPLACEMENT ESTIMATION OF THE GLACIER

This section explores glacier displacement measurement using previous SAR tracking technics. The investigations are made on Argentière and Bossons glaciers for different features. On the one hand, Argentière glacier is instrumented: ground measurements (GPS and "stick" for annual displacement/ablation) allow tracking results evaluation. On the other hand, Bossons glacier is one of the fastest moving glacier of Massif du Mont-Blanc (about 1~m/day) and major part of its surface is textured (cracks): tracking algorithm can provide interesting results.

With complex SAR images, displacement estimation of geophysical objects (fault, mud-slide...) are usually measured by DinSAR. When DInsar is not possible, tracking algorithms like correlation are also used with intensity SAR images. In practice, these techniques only run with large displacement, for example to measure large earthquakes [7][8]. As most of the temperate glaciers are large moving geophysical objects, these techniques may be adequate. There are two main features in tracking algorithms: the cross-correlation and texture tracking algorithms. Cross-correlation maximisation corresponds to the minimisation of the squared difference. It is well suited for images corrupted by additive noise and is often not robust enough for monitoring displacement with SAR images. In the contrary, texture tracking is more accurate and robust for global measurements as soon as it takes multiplicative

noise statistics of SAR imagery (speckle) into account. The particularity of SAR images is to contain point targets in addition to global ground response. These targets can be natural (rocks) or artificial (corner reflector). Then, two approaches are explored: point target and global measurements. Point target approach is applied to artificial target, i.e. corner reflector, using sub-pixel correlation. And the global approach is applied to the natural texture of the scene, i.e. the global surface of glacier, using texture tracking algorithm.

3.1 Methods used for displacement estimation

3.1.1 Point target measurement (*sinc* method) - The impulse response of a SAR system like TerraSAR-X is a cardinal sinus (sinc). This response can be observed in Fig. 1-(b). Francesco Serafino [9] has developed a co-registration method based on the cross-correlation between the ideal impulse response of the system and some isolated point scatterer. With point targets like corner reflectors, the response is very strong and accurate. This technique has been experimented to measure the displacement of the corner reflector installed on the Argentière glacier. In the rest of the article this technique will be called *sinc* method. The sub-pixel position of the corner reflector is extracted from an amplitude TerraSAR-X images pair to determine its displacement. Such method may be decomposed as follow:

- Extract a window in each image containing the corner reflector ,

- Calculate the cross-correlation between each window and the ideal impulse response,

- Over-sample the two results of the cross-correlation,

- Extract the two peaks and differentiate them to find the displacement (in pixel) in range and azimuth direction,

- Subtract sub-pixel co-registration values to the displacement.

3.1.2 Global measurement (*UML* method) - Texture tracking methods have been already used with success to monitor cold and temperate glacier with TSX images [6]. Furthermore, a new texture tracking algorithm has been proposed by Erten and al. [10], and has been successfully tested with ENVISAT-ASAR satellite data to monitor Inyltshik temperate glacier (Kirgyzstan). Supposing two intensity SAR images x and y, this algorithm tries to match the image blocks by maximizing the conditional density function (CDF). The matching result is the shift vector $\vec{v}_i$.

The maximum likelihood (ML) texture tracking estimate v is obtained by maximizing for each block i the CDF function:

$$\vec{v}_{iMLtt} = Arg_v p(x,y,v) \quad \max|, \quad (\quad) \tag{1}$$

In regard to SAR image intensity statistics, with uncorrelated speckle model, maximizing the CDF is equivalent to maximize the following objective function:

$$ml_u(\vec{v}_i) = \sum_{j=1}^{k} \underline{x_{ij}} - \underline{y_{ij}} - 2\ln\left(1 + e^{\left(\underline{x_{ij}} - \underline{y_{ij}}\right)}\right), \qquad \text{where } \underline{x_{ij}} = \ln\left(x_{ij}\right) \text{ and } \underline{y_{ij}} = \ln\left(y_{ij}\right). \tag{2}$$

A new texture tracking function, assuming correlated speckle model, has also been proposed by Erten et al.:

$$ml_c(\vec{v}_i) = \sum_{j=1}^{k} \underline{x_{ij}} - \underline{y_{ij}} - 2\ln\left(1 + e^{\left(\underline{x_{ij}} - \underline{y_{ij}}\right)}\right) - \left(1 + \frac{1}{2N}\right)\ln\left(1 - \frac{4\rho_{ij} e^{\left(\underline{x_{ij}} - \underline{y_{ij}}\right)}}{\left(1 + e^{\left(\underline{x_{ij}} - \underline{y_{ij}}\right)}\right)}\right) \tag{3}$$

where N represents the number of looks and ρ is the correlation coefficient. According to [11], data with correlation below ρ =0.5 may be considered as uncorrelated, and therefore Eq. 2 should be used instead of Eq. 3. The maximization of cross-correlation between two intensity SAR images (Fig. 4-(a)) on Argentière and Bossons glaciers, shows that in this data set, glacier surfaces are uncorrelated after 11 days: the major part of glaciers has a correlation coefficient below ρ =0.5. Therefore, displacement results of next subsection are computed by using Eq. 2. In the rest of the article this method will be called *UML* method.

3.2 Results on Mont-Blanc test area - Argentière and Bossons glaciers

First, this section contains a short description of in situ measurements. After, results of *sinc* and *UML* methods are analyzed. Then, for Argentière glacier, a comparison between remote-sensing measurements and ground truth is realized. Estimation of glacier displacement has been made with 3 TSX images of autumn 2008 (see Tab. 1) owing to GPS measurements available only over this time period. The point target measurements on the CR used sub-pixel co-registration (see part 3.1.1) using RAT (RAdar Tools, software developed by the Computer Vision and Remote Sensing Group of the Berlin University of Technology). The global measurements are computed with data pairs which have been formed with pixel registration (only translation without resampling). For both methods and ground

truths. according to the range and the azimuth pixel spacing, and the time interval, we convert the displacement on centimetre/day in slant range/azimuth geometry.

3.3.1 In situ measurements description - Since summer 2007, three continuous GPS stations are recording in the Argentière glacier area: one site (station code ARGG) in the upper part of the glacier (alt. 2767 m) close to the corner reflector (at 5 m distance), a second site (ARGR) on the bedrock beside the glacier (alt. 2837 m), and a third station (CHMX) in the town of Chamonix down in the valley (alt. 1121 m). In the time interval presented in this work (29/09/2008-21/10/2008, day of year 273-295 of 2008) the three stations have been operational, except for the glacier station that is missing the four last days. The GPS data of these three stations have been combined with continuous GPS data of 42 stations from the French RENAG and RGP and the European EUREF networks (http://renag.unice.fr, http://rgp.ign.fr, http://www.euref-iag.net/) and analyzed with the GAMIT/GLOBK software created at MIT [12]. The data are acquired at a 30 sec interval. We estimate the station coordinates over 6 hour sessions. This results in position time series with four estimates per day. The positioning of the fast moving glacier site with respect to the stable reference stations is estimated with formal uncertainties of 2-3 mm on the horizontal components and 9-11 mm on the vertical component for each 6 hour session. These positions can be used to determine a linear displacement rate over the total observation span (18 days for the glacier sites missing the last four days), or over sub-intervals between the successive satellite image acquisition dates (12 and 6 days for the glacier site). In a second analysis step we estimate tropospheric parameters with a high temporal resolution (one zenith tropospheric delay every 15 min). Here we use a sliding window strategy shifting 8 six-hour sessions per day by 3 hours and keeping only the results from the central 3 hour interval of each solution.
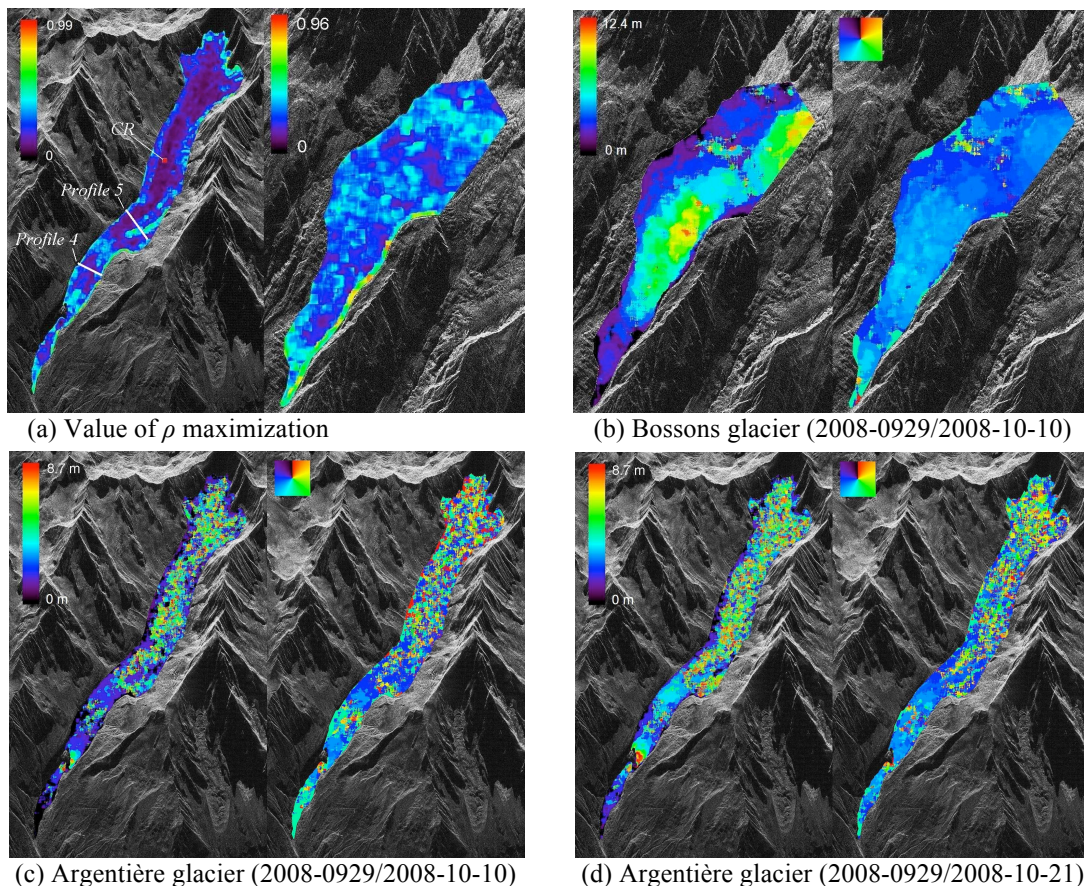

(a) Value of ρ maximization

(b) Bossons glacier (2008-0929/2008-10-10)

(c) Argentière glacier (2008-0929/2008-10-10)

(d) Argentière glacier (2008-0929/2008-10-21)

Figure 4. (a) Value of correlation maximization for Argentière and Bossons glaciers with 2008-0929/2008-10-10 pair. (b) Bossons and (c)/(d) Argentière glaciers slant range/azimuth geometry displacement estimation (magnitude and orientation), computed with *UML* method (Eq.~(2)). (b) and (c) correspond to the 2008-09-29/2008-10-10 pair and (d) to the 2008-09-29/2008-10-21 pair. All results are computed with 51×51 pixels block size.

The second source of in-situ measurements comes from "ablation sticks" installed on several parts of Argentière glacier for annual displacement and mass-balance measurements. Consequently, measurement is biased by the

displacement variations along year°: larger during the hot season, reduced during the cold season. Several displacement profiles, i.e. 5 stick border to border, are made across the glacier by the LGGE (Laboratoire de Glaciologie et Géophysique de l'Environnement). The sticks at center of glacier and two profiles may be used for comparison: profiles 4 and 5 (see Fig. 4-(a)) because they correspond to lower part of Argentière glacier where *UML* method runs.

   3.3.2 Analysis of results and comparison with ground truth - Tab. 2 shows the CR displacement which is measured by the *sinc* method. The results show that displacement estimation with 2008-10-10/2008-10-21 pair is higher than the other two pairs°: there is a relative deviation of *~60%*. Considering that the three images are acquired at the same period of the year, the results should be homogeneous. This anomaly may be caused by co-registration rather and the relatively short time interval between images used to form pair; in this part of the glacier during 11-days the displacement is short, consequently a co-registration error may be create significant measurement error.

   Displacements of Bossons and Argentière glaciers computed with *UML* method are shown respectively in Fig. 4-(b) and 4-(c)/(d). For each result, magnitude and orientation of displacement vector are calculated. The displacement estimation of Bossons glacier (Fig. 4-(b)) shows typical displacement pattern of glacier with the highest displacement in the center of the glacier and a gradient towards the boundary. Furthermore, two zones with largest displacement correspond to increasing slope. The cracked surface of Bossons glacier explains this relatively good result. In contrary, the displacement estimation of upper part of Argentière glacier (Fig. 4-(c) and 4-(d)) is damaged by noise. This noise is created by surface texture de-correlation due to snowfalls. The displacement map of the lower part of Argentière glacier shows more reliable results. The two data set pairs, 2008-09-29/2008-10-10 and 2008-09-29/2008-10-21, show the large glacier displacement caused to "Lognan serac falls". The presence of breaking slope explains it. Displacement map comparison of two data pairs (11-day and 22-day) reveals, on the center of the lower part of the glacier, a displacement multiplied by two. Nonetheless, because the co-registration maximum is not interpolated, the displacement map of 2008-09-29/2008-10-10 pair shows no motion areas. In fact these areas have sub-pixel motion which will be estimated by a refined version of the tracking algorithm.

   Tab. 2 lists displacement measurements obtained on Argentière glacier according to localization on the glacier. All of them are shwon in slant range/azimuth geometry to make easier comparison. Overall, CR displacements estimation by *sinc* and *UML* methods are close to GPS results. But, for each method, one pair shows a value far away the GPS°: 2008-09-29/2008-10-10 and 2008-10-10/2008-10-21 respectively for *UML* and *sinc* methods. This happen due to the pixel co-registration problem. At the center of the profiles 4 and 5, *UML* method allows good displacements estimation°: they are close to "ablation stick" measurements. However, this comparison requires being careful because sticks measurements are annual.

Table 2. Comparison between ground and remote-sensing (*italic*) measurements of displacements according to measurements position on Argentière glacier (see Fig 4-(a)). All results are put in slant range/azimuth geometry on cm/day .

Δt	Displacement cm/day	CR (2700 m)			Profile 5 (2550m)		Profile 4 (2380 m)	
		GPS*	*sinc*	*UML*	stick	*UML*	stick	*UML*
11 days	2008-09-29/2008-10-10	8.5	*8.9*	*0.0*	-	*13.6*	-	*15.9*
	2008-10-10/2008-10-21	8.4	*14.9*	*8.2*	-	*13.6*	-	*15.9*
22 days	2008-09-29/2008-10-21	8.4	*9.3*	*7.9*	-	*13.6*	-	*15.9*
1 year	2006-09-06/2007-09-05	-	-	-	10.9	-	17.0	-

*(*at 5 m distance of CR).*

CONCLUSION AND PERSPECTIVES

   In this paper, the early results obtained with multi-temporal TerraSAR-X images over Chamonix Mont-Blanc glaciers have been presented and compared with in-situ measurements.

   Regarding the phase information, the analysis of several autumn and winter 11-day interferograms allows to conclude that on white glaciers (ice/snow covered) surface changes are too important to obtain regularly coherence and phase information, whereas on black glaciers (covered by stones), or in intermediate areas, coherence can be high enough to observe displacement fringes. However, the moving parts of such glaciers have to be carefully

registered in order to preserve this information: with the TSX HR data, on fast moving glaciers, the global registration obtained on non-moving well correlated areas may result in important miss-registration over the glacier. The use of prior information on the glacier location and displacement should be investigated to respond to this specific requirement on sparse, poorly correlated, moving areas.

Regarding the intensity information, the gain in resolution makes the observation of important Alpine glacier features feasible: large stones, crevasses, seracs... Due to their increased visibility and the meter resolution, the displacement of fast moving glaciers can also be measured on the intensity by ``correlation like'' methods. Two different kinds of feature have been successfully tracked: point target features with an artificial target (a moving corner reflector) and texture features. These first results have been compared with in-situ measurements (a continuous GPS located near the CR and ablation sticks). They show that both approaches are feasible and complementary°: displacement estimation by texture tracking works only with textured area, i.e. cracked areas or in the presence of stones, whereas the *sinc* method approach works on isolated point targets.

Further work is necessary to refine the different methods using multi-temporal SAR images in order to derive displacement with higher accuracy and to assess the uncertainty of the different approaches. It will include the fusion of the different information sources, especially a combined use of SAR and GPS data. Since the GPS tropospheric delays are equivalent to the tropospheric delays affecting the satellite radar images, the GPS network can be used to correct this persistent error in SAR imagery. The tropospheric variability in the atmospheric layers as observed by our GPS stations (1121m-2767m and 2767m-2837m) offers interesting perspective for the development of SAR tropospheric corrections from GPS observations.

Acknowledgements

REFERENCES

[1]   E. Berthier, H. Vadon, D. Baratoux, Y. Arnaud, C. Vincent, K.L. Feigl, F. Rémy, and B. Legrésy. Mountain glaciers surface motion derived from satellite optical imagery. *Remote Sensing Environ.*, 95(1):14–28, 2005.

[2]   E. Trouvé, G. Vasile, M. Gay, L. Bombrun, P. Grussenmeyer, T. Landes, J.M. Nicolas, P. Bolon, I. Petillot, A. Julea, L. Valet, J. Chanussot, and M. Koehl. Combining airborne photographs and spaceborne SAR data to monitor temperate glaciers. Potentials and limits. *IEEE Transactions on Geoscience and Remote Sensing*, 45(4):905–923, 2007.

[3]   T. Landes, M. Gay, E. Trouvé, J.-M. Nicolas, L. Bombrun, G. Vasile, and I. Hajnsek. Monitoring temperate glaciers by high resolution Pol-Insar data: first analysis of argentière E-SAR acquisitions and in-situ measurements. *IEEE Geoscience and Remote Sensing SymposiumProceedings*, *IGARSS'07*, Barcelona, Spain, 2007.

[4]   TerraSAR-X science service system: Proposals Pre-launch. http://sss.terrasar-x.dlr.de.

[5]   V. Kumar, G. Venkataraman, Y.-S. Rao, and G. Singh. Glacier movement study in NW-Himalayan region using repeat pass high resolution TerraSAR-X data. In *TerraSAR-X Science Team Meeting*, *Oberpfaffenhofen*, *Germany*, 2008.

[6]   D. Floricioiu, K. Jezek, K. Farness, M. Eineder, N. Yague-Martinez, H. Rott, and H. Björnsson. TerraSAR-X observations of ice velocities in Antartica, Patagonia and Iceland. In *TerraSAR-X Science Team Meeting*, *Oberpfaffenhofen*, *Germany*, 2008.

[7]   T.J. Wright, E. Barry, E. Parsons, and Zhong Lu. Toward mapping surface deformation in three dimensions using InSAR. *Geophysical Research Letters*, 31, 2004.

[8]   E. Pathier, E.J. Fielding, T.J. Wright, R. Walker, B.E. Parsons, and S. Hensley. Displacement field and slip distribution of the 2005 Kashmir earthquake from sar imagery. *Geophysical Research Letters*, 33, 2006.

[9]   F. Serafino. Sar Image Coregistration Based on Isolated Point Scatterers. *IEEE Geoscience and Remote Sensing Letters*, 3(3):354–358, 2006.

[10]   E. Erten, A. Reigber, and O. Hellwich. Glacier velocity monitoring by maximum likehood texture tracking. *IEEE Transactions on Geoscience and Remote Sensing*, 47(2):394–405, 2009.

[11]   F. Chatelain, J.Y. Tourneret, J. Inglada, and A. Ferrari. Bivariate gamma distributions for image registration and change detection. *IEEE Trans. on Image Processing*, 16(7):1796–1806, 2007.

[12]   T.A. Herring, R.W. King, and S.C. Mc. Clusky. GAMIT Reference Manual. GPS Analysis at MIT Release 10.3, Department of Earth, Atmospheric and Planetary Sciences, Massachusetts Institute of Technology, 2006.